UCRL- 95373
PREPRINT

Nuclear De-Excitation Processes Following Medium Energy Heavy Ion Collisions

UCRL--95373

DE87 000600

M. Blann

This paper was prepared for submittal to
the Proceedings of the
School on Heavy Ion Physics
Dubna, USSR

September 1986

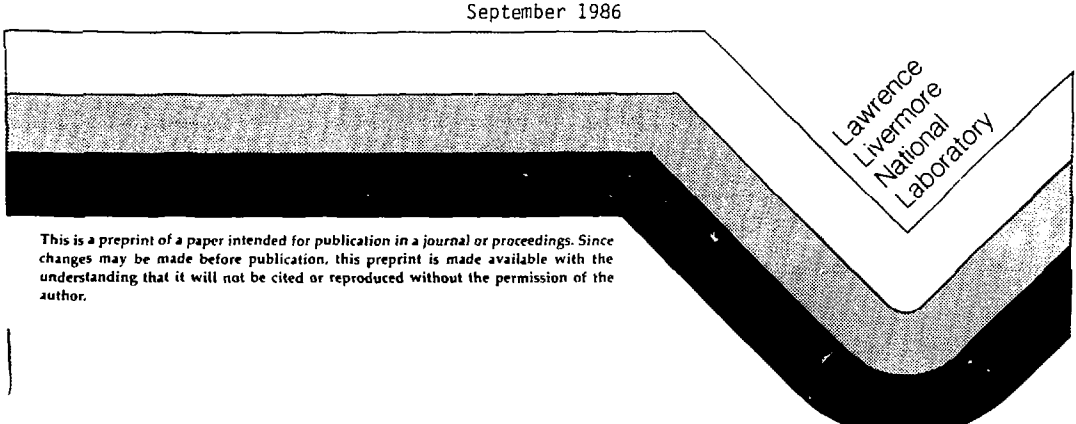

DISCLAIMER

NUCLEAR DE-EXCITATION PROCESSES FOLLOWING MEDIUM ENERGY HEAVY ION COLLISIONS

M. Blann
Lawrence Livermore National Laboratory
University of California
Livermore, California, U.S.A.

I. Introduction

As heavy ion reaction studies have progressed from beam energies below 10 MeV/nucleon to higher energies, many non-equilibrium reaction phenomena have been observed. Among these are nucleon emission with velocities in excess of the beam velocity,[1-3] incomplete momentum transfer to evaporation residue and fission-like fragments,[4] γ-rays with energies in excess of 100 MeV,[5,6] and π^0 production when beam energies are below the threshold for production by the nucleon-nucleon collision mechanism.[7-10] Additionally, prefission neutrons have been observed in excess of numbers expected from equilibrium models.[11,12]

We try to understand and interpret these phenomena in terms of models or theories. A few of the approaches which have been applied to these phenomena are as follows:

1. Intranuclear cascade: Two body collisions are assumed to mediate the equilibration. The geometry and momentum space is followed semiclassically. The approach has many successes though it may suffer in a few applications in not following "holes." We refer interested parties to some of the excellent papers in the literature for further discussion of the INC model as applied to heavy ion reactions.[13]

2. TDHF considers one body processes only; in the energy regime of interest, two body processes are important so that this may not be a viable approach.

3. Boltzmann-Uehling-Uhlenbeck or Vlasov-Uehling-Uhlenbeck (BUU/VUU) equations combine both one body and two body dynamics. The spatial and momentum evolution of the reactions are followed in a mean field. These should be the Cadillacs of the models. They are computationally tedious, and sometimes significant approximations are made in order to achieve computational tractability. Work on developing these models has been done by Bertsch, Aichelin, Stöcker and their collaborators.[2]

4. Models of collective deceleration. Such an approach for γ-ray and π^0 production by a bremsstrahlung mechanism has been introduced by Vasak, Müller and Greiner.[15]

Here I shall discuss a very simple model approach to interpret these phenomena, the Boltzmann master equation (BME).[16,17] The hybrid model was the first to be applied to the question of heavy ion precompound decay, and the BME second.[18] Both approaches follow the nuclear relaxation process as proceeding in a central potential by a series of two body (nucleon-nucleon) scattering processes, mediated by the Pauli exclusion principle and continuum emission.

I shall describe the physical concepts of the BME and summarize the numerical formulation (II). Next, I shall summarize the success in reproducing experimental (HI,n) spectra and in estimating limits on beam momentum transfer due to the precompound nucleon emission cascade (III). Results of calculations for subthreshold pion production will be presented and compared with experimental yields (IV), and I shall then summarize the value of this simple model approach in the interpretation of these precompound phenomena (V).

II. Formulation of the Boltman Master Equation

The concepts of the BME are represented in Fig. 1, where it may be seen that for a given energy bin in the nuclear potential, we explicitly calculate the rates of scattering into, out of, and continuum emission from a bin of interest. The population readjustment versus time is mediated solely by two body N-N collision processes based on free N-N scattering cross-sections and the Pauli exclusion principle. The set of master equations may be represented by:[16,17]

$$\frac{dn_i^p}{dt} = \sum_{jkl}[\omega_{ij\to kl}^{pp} g_i^p g_j^p g_k^p n_k^p n_l^p (1-n_i^p)(1-n_j^p)] - [\omega_{ij\to kl}^{pp} g_i^p g_j^p g_k^p n_i^p n_j^p (1-n_k^p)(1-n_l^p)]\delta(\epsilon_i^p+\epsilon_j^p-\epsilon_k^p-\epsilon_l^p) \quad \text{(Eq. 1)}$$

$$+\sum_{jkl}[\omega_{ij\to kl}^{pn} g_i^p g_j^n g_k^p n_k^p n_l^n (1-n_i^p)(1-n_j^n) - \omega_{ij\to kl}^{pn} g_i^p g_j^n g_k^p n_i^p n_j^n (1-n_k^p)(1-n_l^n)]\delta(\epsilon_i^p+\epsilon_j^n-\epsilon_k^p-\epsilon_l^n)$$

$$-n_i^p \omega_{i\to i'}^p g_{i'}^p \delta(\epsilon_i^p-\epsilon_{i'}^p+\epsilon_f^p+B_p)\,,\quad i=1,\ldots,\epsilon_f^p+E^*\,,\quad i'=1,\ldots,E^*-B_p\,, + \frac{dfus}{dT}$$

with an analogous expression for neutron population relaxation processes. The dfus/dt term is a source term, representing a time dependent injection of nucleons and excitation energy during the coalescence (fusion) process; this term will be discussed shortly.

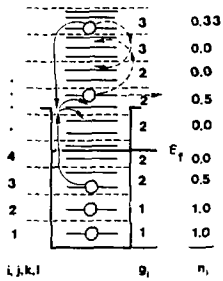

Figure 1. Representation of a Fermi gas nucleus as treated in the Boltzmann master equation. The nucleus is divided into 1 MeV wide energy bins, indexed by i, j, k or l counting from the bottom of the Fermi sea. The number of single particle levels, g_i per MeV is calculated, and the occupation probability n_i is also followed. The rate of scattering into and out of each bin (and if energetically allowed, of emission into the continuum) is calculated for a time interval less than the nucleon-nucleon collision period; all nucleon populations are appropriately modified after each time interval. The Pauli exclusion principle is treated by the $(1-n_i)$ terms (Eq. 1).

The Pauli exclusion operators may be seen in the BME as the $(1-n_i)$ terms, giving the fraction empty of final bins. The symbols of the BME are summarized in Table 1. The rate of scattering of two nucleons at energies i and j into final energies k and l is given by:[4]

$$\omega_{ij\to kl}^{pp} = \frac{\sigma^{pp}(\epsilon_i^p+\epsilon_j^p)[(2/M)(\epsilon_i^p+\epsilon_j^p)]^{1/2}}{V\sum_{mn}' g_m^p g_n^p \sigma^{pp}(\epsilon_i^p+\epsilon_j^p-\epsilon_m^p-\epsilon_n^p)}\,, \quad \text{(Eq. 2)}$$

A more thorough discussion of the BME, as encoded originally by Harp, Miller, and Berne, and later modified by Blann, may be found in Refs. 6 and 7.

There is still the question of the rate and energy distribution of nucleons injected during coalescence in a heavy ion reaction, the source term of Eq. 1. How to calculate and model this is a very interesting, very much open question. In the limit of a light projectile on a heavy target we might expect a random, energy conserving distribution, with degrees of freedom (n-1) approximately equal to the projectile mass, A_p, as was found useful in reproducing (α,N) spectra in the hybrid precompound decay model.[18] One way of testing this notion is by

using the BME with an initial exciton population given by such an equal a-priori probability distribution, with the initial exciton number n taken as a free parameter, selected to give a best fit to experimental fusion gated spectra. This has been done by the Berlin[2,3] and Zagreb groups.[19] Results are summarized in Fig. 2, based on a figure from Refs. 3 and 19, where values of n from A_p-1 to A_p+8 were found for a very wide range of projectiles. The narrow range of n values tends to support the basic idea that the reactions may be described as proceeding through a number of degrees of freedom closely associated with the projectile mass. The early data seemed to show a strong energy dependence of the value extracted for the n parameter; however, note in Fig. 2 that the recent 25 MeV/nucleon ^{12}C point of the Berlin group[3] implies a more nearly constant value of n. Indeed, we will show that we can satisfactorily fit all the Berlin Ne and 25 MeV/nucleon ^{12}C results satisfactorily with $n \approx A_p$ and with no modification of the nucleon-nucleon mean free paths. This is an empirical observation, not a theoretically predicted result. The energy distribution of nucleons so calculated is assumed to be injected as the fraction of the projectile sphere which would pass through a plane per time increment, at a velocity equal to the beam velocity reduced for the coulomb barrier.

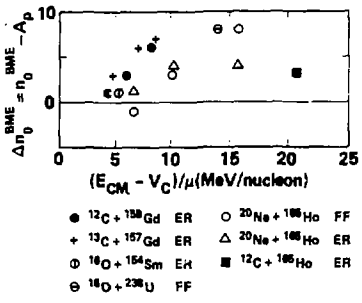

Figure 2. Degrees of freedom deduced for several heavy ion induced reactions by varying the n parameter in the BME. This figure is taken from Refs. 3 and 19. The ordinate gives the difference between the best fit n parameter of the Ericson expression as used for the initial exciton distribution in the BME injection term, and the projectile mass number A_p. The abscissa gives the projectile energy in MeV/nucleon (cm) above the coulomb barrier. The choices of target and projectile are given in the legend. Sources of original data are given in Ref. 19.

The course comparisons of n in Fig. 2 are encouraging, and we owe thanks to the Berlin and Zagreb groups for exploring this important parameter of the BME approach; for the future we must consider putting a little more physics into the coalescence distribution function. For example, including higher partial waves than ℓ=0 will tend to reduce the energy dependence noted for the n parameter. Similarly, the distribution function should be limited to maximum and minimum nucleon energies as given by the relative and Fermi velocities (as is done for calculation of the π^0 production cross sections discussed in III.C). Accessible cells in phase space rather than equipartition based on energy should also be considered. We are looking into these possibilities at present, and hope to have results in the near future.

Next, we compare the BME using the Ericson input distribution function with experimental (HI,n) spectra. This will be followed by comparisons with predictions for π^0 production, for which case the distribution function must be calculated with constraints on maximum nucleon energies.

III. Comparisons of Calculated and Experimental Results

A. (HI,n) Spectra

In Fig. 3, we show comparisons between evaporation residue (ER) and fission fragment (FF) gated, angle integrated neutron spectra from the ^{20}Ne bombardment of ^{165}Ho. The "experimental results" are parameterized calculated points for

the "fast" component. These data were fitted by the Berlin group with the BME with n values of 20-24 (ER gated spectra) and 20-28 (FF gated spectra) with the average nucleon mean free path being twice the result due to N-N scattering processes. We show calculated results for these spectra using n=20 and 23 without modification of the nucleon mfp.[17] The value of n=20 seems to give a satisfactory fit to all the data, within the uncertainties stated previously on the "primal" distribution function used, and somewhat even based on uncertainties in the angle integration method used on the data. I should emphasize that the absolute values of the calculated spectra are compared with the experimental results in Fig. 3 without any normalization, and are all calculated without adjustment of the nucleon-nucleon mean free path.

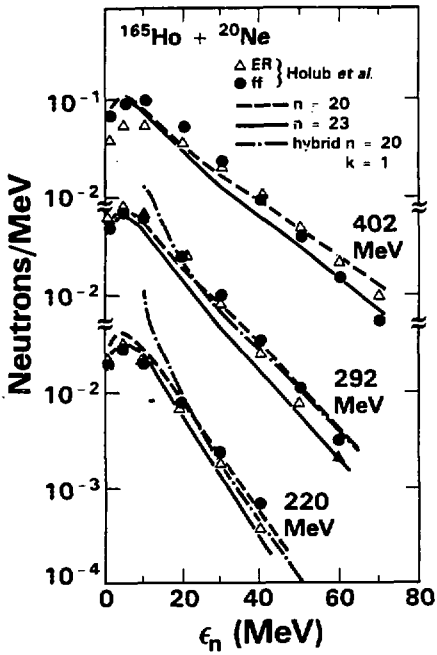

Figure 3. Calculated and experimentally deduced spectra for the $^{165}Ho(^{20}Ne,n)$ reaction at laboratory energies of 220, 292, and 402 MeV. Experimental points from Ref. 2 result from an integration of a moving source fit to experimental yields for the fast component only. Experimental yields were gated on evaporation residues (ER) as represented by open triangles, and on fission fragments (FF) shown by closed circles. Calculated results are shown for the BME with n of Eq. 1 taken as 20 and 23, and for a hybrid model calculation with n=20.

Recently the Berlin group has measured $^{165}Ho(^{12}C,n)$ at 25 MeV/nucleon incident energy.[3] Results are shown in Fig. 4. They found excellent agreement with experimental spectra with n=15, k=4, as shown. We get satisfactory agreement for n=12, k=1. The BME may be seen to give a quite satisfactory agreement for an a-priori calculation over a broad range of incident energies and projectiles, yielding spectra correct in shape and magnitude, without normalization of the spectral intensities.

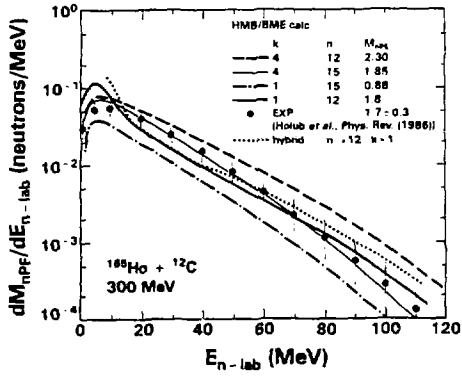

Figure 4. Calculated and experimentally deduced neutron spectra for the ^{165}Ho (^{12}C,n) reaction at 25 MeV/nucleon. The data were angle integrated as for Fig. 3; these results are from Ref. 3. Several spectra calculated with the BME in Ref. 3 are shown. To these, we have added results of the BME for n=12, k (meanfree path multiplier) =1, and a result with the hybrid mode) from code ALICE for n=12, k=1.

In Figs. 3 and 4, we also see the result of a calculation using the hybrid model via the code ALICE. Here too, for k=1 and n=A_p, the calculated spectra are in quite good agreement with the experimentally deduced results. The disagreement at lower channel energies results because the ALICE calculation includes equilibrium components, while the experimental representation has excluded these.

The BME seems to give a reasonable representation of the nucleonic cascade. Could the linear momentum removed by the nucleons account for the linear momentum decrement observed in many experiments? This can be calculated if we know something of the angular distribution of the emitted nucleons.

B. Linear Momentum Transfer

Rather than performing a sophisticated calculation of nucleon angular distributions, or better yet, inputting algorithms based on experimental results, we have assumed nucleon emission at an energy dependent angle based on a Heisenberg type of limit,

$$R\Delta\theta \geq 2\pi/k \quad , \qquad \text{(Eq. 3)}$$

a result based on earlier work of Mantzouranis, et al.[20] This algorithm was shown to be useful in the case of (N,N') angular distributions.[21] Eventually, a more sophisticated approach should be taken. Nonetheless, this limit should give a rough estimate of the momentum removed by the nucleonic cascade. Results of momentum transfer calculations for $^{16}O+^{60}Ni$ and $^{27}Al+^{86}Kr$ are shown in Fig. 5. Some experimental results, due to many workers, as summarized by Chan et al.,[4] are also shown. Overall, the agreement between calculated and experimental results is quite good, but there are some very big caveats. First, in a more detailed comparison at the lower incident energy end of the curve, Viola finds that the BME overestimates the linear momentum decrement.[22] Secondly, there is some evidence that at the higher bombarding energies, a significant part of the linear momentum decrement may be due to cluster emission.[23] While our calculation makes a small allowance for this, some experiments suggest that nature may be providing many more clusters per interaction. The only reason for hedging this statement at all is that some of these experimental measurements have instrumental cutoffs of the low energy protons, so that a proper estimate of cluster vs. nucleon emission multiplicities is still somewhat ambiguous.

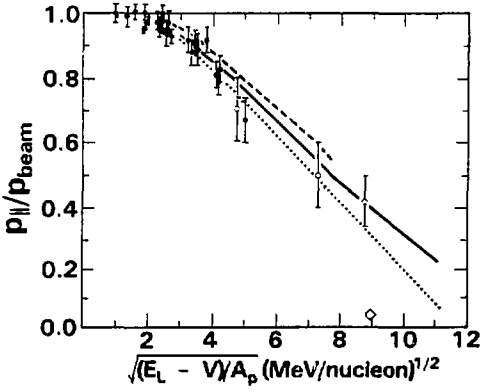

Figure 5. Calculated and experimental results for the fraction of beam linear momentum transferred ($p_{\parallel}/p_{beam}$) in heavy ion reactions versus laboratory velocity in excess of the coulomb barrier. The experimental values shown are from a compilation due to Yuen-Dat Chan (Ref. 4). The dotted curve is a calculated BME result for $^{60}Ni+^{16}O$ assuming n=16, with a lower limit of nucleon injection energy above ϵ_F of $(\sqrt{\epsilon_F} - \sqrt{\epsilon_F})^2$. The solid line is for $^{60}Ni + ^{16}O$ assuming n=19, and the dashed line is for $^{27}Al + ^{86}Kr$ assuming n=30.

Perhaps this is a good point to emphasize that linear momentum transfer is not a very unambiguous probe of models such as the BME. Rather the ER or FF gated nucleon or cluster emission spectra provide a more stringent test. For the available nucleon emission data the BME is doing well for relatively few data; what is needed is a broader data base. Measurement of the very high energy end of the nucleon spectra would be especially interesting, particularly as it relates to the assumed mechanism of coupling nucleon relative momenta with Fermi momenta in the injection/coalescence process. This point is in turn of particular interest to N-N collision explanations for subthreshold pion production. In this regard, the (^{12}C,n) data of Fig. 4 are particularly interesting, for they show the presence of high energy nucleons capable of producing pions via the N-N collision process.

C. Subthreshold Pion Production

Early on, Bertsch[24] suggested that the Fermi momentum and relative nucleon motion might couple in heavy ion reactions to give nucleons sufficient energy to produce pions via a N-N collision mechanism. Arndt and VerWest have tabulated excitation functions for N+N → N+N + pion.[18] We should be able to add these channels to the BME to probe the possibility of the N-N collision process as a viable subthreshold pion production mechanism.[25] The input nucleon spectra for these calculations have been calculated with all energy partitions equally likely, but with no exciton having more than $(\sqrt{\epsilon_F} + \sqrt{\epsilon_F})^2$ units of energy where ϵ_F is the projectile Fermi energy and ϵ_r is the relative energy *per nucleon*. We assumed $n=A_p$ which, recalling the recent Berlin results (Fig. 4), gave excellent agreement between calculated and measured nucleon spectra in the pion production energy range. The rate equations for pions may be represented by:[25]

$$\frac{dN^{\pi}}{dt} = \sum_{ijk'l'm} \omega_{ij}^{pp\pi^0}{}_{k'l'm} g_m g_i^p g_j^p n_i^p n_j^p (1-n_k^p)(1-n_l^p) \qquad \text{(Eq. 4)}$$

$$+ \sum_{ijk'l'm} \omega_{ij}^{pn\pi^0} g_m g_i^p g_j^n n_i^p n_j^n (1-n_k^p)(1-n_l^n)$$

$$+ \sum_{ijk'l'm} \omega_{ij}^{nn\pi^0} g_m g_i^n g_j^n n_i^n n_j^n (1-n_k^n)(1-n_l^n),$$

with the collision rate expressions given by:[19]

$$\omega_{ij\to k'l'm}^{pp\pi^0} = \frac{\sigma^{pp\pi^0}(\epsilon_i+\epsilon_j)[(2/M)(\epsilon_i^p+\epsilon_j^p)]^{1/2}}{V\sum_{n\ell p}' g_n g_\ell g_p \delta(\epsilon_i^p+\epsilon_j^p-\epsilon_k^p-\epsilon_\ell^n-\epsilon_p^\pi-m_{\pi^0})} \quad \text{(Eq. 5)}$$

We use the experimental NNπ^0 production rates due to Verwest and Arndt.[26] Results of these calculations via the BME for a fairly broad range of experimentally measured systems are summarized in Table 2. The calculated yields include a crude π^0 emission attenuation factor estimated for a 2 Fm mean free path. More details may be found in Ref. 25. The results are also quite sensitive to the value of the Fermi energy assumed for the projectile, which was 35 MeV in all cases. We might, for example, expect lower values for the lightest projectiles. In view of the uncertainties of these calculations, we subjectively feel that agreement within a factor of 3-4 between calculated and measured yields is confirmation that the N-N collision is one (but by no means the only) viable mechanism for subthreshold pion production. This is seen to be the case for all the systems summarized in Table 2, except $^{40}Ca+^{40}Ar$, where the discrepancy is a factor of five, and for the 25 MeV/nucleon data. For the latter, we reasonably reproduce the O+Ni data if we assume a target Fermi energy of 30 MeV. Even this fails for the O+Al case. This, however, does not exclude the N-N mechanism, it merely requires larger collision angles than the 90° assumed in the present application of the BME. For alternative explanations one should e.g., read the interesting nucleus-nucleus bremsstrahlung model due to Greiner and his collaborators.

IV. Conclusions

The BME (and hybrid model) are transparent in the physics used to treat the equilibration process, specifically, a series of N-N collisions generated by free scattering cross-sections and the Pauli exclusion principle. The BME, in particular, is very versatile and it is easy to use to test ideas; e.g., pion production cross-sections, incomplete momentum transfer. The model works quite well in reproducing nucleon emission spectra for central collision processes using an input distribution based on $n \simeq A_p$. More work needs to be done in modeling the initial distribution function with the coupling constraints, phase space constraints, and with consideration of angular momentum averaging.

A broader range (projectile and projectile energy variations) of nucleon and cluster emission spectra gated on central collisions would be welcome as a more severe test of the BME and other precompound decay models. Measurement of nucleons at the highest kinetic energies may give crucial information on the microscopic details of the coalescence process, in particular the coupling of the relative motion and Fermi motion of the projectile nucleons, and of the viability of the N-N collision process for subthreshold pion production.

All caveats considered, these simple precompound decay models yield a wealth of insight into the dynamics of heavy ion reactions. Many of the predictions, made as early as 1974 by use of these models,[18] are now being realized in experimental measurements. These models should continue to be strong tools in the interpretation of heavy ion reactions, especially as more attention is paid to the injection term.

Table I. Definition of Symbols

Symbol	Definition
$n_i^X \omega_{i\to c}^X$	Fraction of population of the nucleons of type X (neutron=n, proton=p) emitted per unit time from a bin at energy i measured from the bottom of the Fermi sea.
$\omega_{ij\to kl}^{XY}$	Rate at which one nucleon of type X at energy i scatters with one nucleon of type Y at energy j into final energies k and l.
g_i^X	Number of states for a particle of type X in a 1 MeV wide energy bin centered at energy i with respect to the Fermi energy.
n_i^X	Fraction of the g_i^X levels in bin i which are occupied at time t.
B_X	Binding energy of a nucleon of type X.
ϵ_i^X	Single particle energy of a nucleon of type X in bin i, measured from the bottom of the Fermi sea.
$\omega_{i\to c}^X$	Rate at which a particle of type X at energy i with respect to the bottom of the nucleon well and energy i' with respect to the unbound continuum is emitted into the continuum.
$\delta(\epsilon_i^X+\epsilon_j^Y-\epsilon_k^X-\epsilon_l^Y)$	Unity when initial and final nucleon energies conserve energy, otherwise zero.
E^*	Composite system excitation energy.
V	The nuclear volume, calculated in this work using a square well with radius parameter 1.2×10^{-13} fm.
M	Nucleon mass.
$\sigma^{XY}(\epsilon_i+\epsilon_j)$	Cross section for a free nucleon of type X and energy ϵ_i to collide elastically with a free nucleon of type Y and energy ϵ_j.
$\sigma^{XY\pi^0}(\epsilon_i+\epsilon_j)$	Cross section for a nucleon of type X at energy ϵ_i to collide with a nucleon of type Y at energy ϵ_j to produce a π^0 plus nucleons X and Y with final energies such that mass and energy are conserved.

Table II. Summary of Calculated and Experimental Subthreshold Pion Production Cross-Sections

Projectile Target	MeV Nucleon	Calc. Expt.	Expt. σ_{π^0}(μb)	Emitted[a] Calc. σ_{π^0}(μb)	Ref. Exptl.	Calc. f_{atten}	E*(MeV)
$^{12}C/^{238}U$	84	0.6	174.(27)	110.	b	0.24	936
$^{12}C/^{58}Ni$	84	2.4	72.(9)	175.	b	0.34	835
$^{12}C/^{12}C$	84	0.7	19.(23)	14.	b	0.42	518
$^{12}C/^{238}U$	74	0.7	64.(10)	46.	b	0.24	821
$^{12}C/^{58}Ni$	74	2.4	31.(4)	74.	b	0.34	736
$^{12}C/^{12}C$	74	1.6	8.5(10)	14.	b	0.42	458
$^{12}C/^{238}U$	60	0.7	13.(2)	9.2	b	0.24	661
$^{12}C/^{58}Ni$	60	0.6	19.(23)	11.	b	0.34	597
$^{12}C/^{12}C$	60	0.8	1.7(3)	1.4	b	0.42	374
$^{40}Ar/^{238}U$	44	0.5	6.(3)	2.9	c	0.23	1375
$^{40}Ar/^{119}Sn$	44	0.7	3.7(8)	2.6	c	0.27	1257
$^{40}Ar/^{40}Ca$	44	0.2	2.2(4)	0.33	c	0.33	880
$^{14}N/^{184}W$	35	0.4	0.160(20)	0.058	d	0.26	440
$^{14}N/^{58}Ni$	35	0.5	0.120(15)	0.061	d	0.34	395
$^{14}N/^{27}Al$	35	0.4	0.070(10)	0.028	d	0.38	344
$^{16}O/^{58}Ni$	25	0.04	0.0023	0.001	e	0.30	311
$^{16}O/^{58}Ni$	25	0.3	0.0023	0.0006[f]	e	0.30	311
$^{16}O/^{27}Al$	25	0.08	0.0013	0.0001[f,g]	e	0.37	265

a) Calculated as product of calculated pions/interaction times σ_R times f_{atten}, where $\sigma_R=\{1.2(A_T^{1/3}+A_p^{1/3})\times10^{-13}\}^2\pi$, with A_T and A_p target and projectile mass numbers.

b) H. Noll et al., Phys. Rev. Lett. 48, 732 (1982).
c) H. Heckwolf et al., Z. Phys. A 315, 43 (1984).
d) J. Stachel et al., in Proceedings of the Inst. for Nuclear Studies, RIKEN Symposium on Heavy Ion Physics, Tokyo Japan (1984) unpublished.
e) G. R. Young et al., Phys. Rev. C 33, 742 (1986).
f) Calculated assuming a target Fermi energy of 30 MeV.
g) This experimental excitation is below the threshold for N-N production in a 90° collision. The calculated yield is an artifact of following probability flux rather than individual nucleon populations.

References

1. T. C. Awes et al., Phys. Rev. C 25, 2361 (1982).

2. E. Holub, et al., Phys. Rev. C 28, 252 (1983).

3. E. Holub, et al., Phys. Rev. C 33, 143 (1986).

4. Y. D. Chan, et al., Phys. Rev. C 27, 447 (1983).

5. E. Grosse, International Workshop on Gross Properties of Nuclei, Hirschegg (1985); P. Grimm and E. Grosse, preprint GSI-85-50 (1985) unpublished.

6. J. Stevenson et al., Phys. Rev. Lett. 56, 555 (1986); N. Alamanos et al., Phys. Lett. B 174, 392 (1986).

7. H. Noll et al., Phys. Rev. Lett. 48, 732 (1982).

8. J. Stachel et al., in Proceedings of the Institute for Nuclear Studies, RIKEN Symposium on Heavy Ion Physics, Tokyo, Japan (1984) unpublished.

9. H. Heckwolf et al., Z. Phys. A 315, 43 (1984).

10. G. R. Young et al., Phys. Rev. C 33, 742 (1986).

11. A. Gavron et al., Phys. Lett. B (in press).

12. D. J. Hinde et al., Nucl. Phys. A452, 550 (1986).

13. Z. Fraenkel, Nucl. Phys. A 428, 373 (1984).

14. G. Bertsch, in "Frontiers in Nuclear Dynamics," ed. by R. A. Broglia and C. H. Dasso (Plenum Press, 1985), p. 277; J. Aichelin, Phys. Rev. C 33, 537 (1986); J. J. Molitaris and H. Stöcker, Phys. Rev. C 32, 346 (1985).

15. D. Vasak, H. Stöcker, B. Müller and W. Greiner, Phys. Lett. 93B, 243 (1980), and D. Vasak, B. Müller and W. Greiner, Physica Scripta 22, 25 (1980); D. Vasak, W. Greiner, B. Müller, T. Stahl and M. Uhlig, Nucl. Phys. A428, 291c (1984); D. Vasak, B. Müller and W. Greiner, J. Phys. G11, 1309 (1985).

16. G. D. Harp, J. M. Miller and B. G. Berne, Phys. Rev. 165, 1166 (1968); G. D. Harp and J. M. Miller, Phys. Rev. C 3, 1847 (1971).

17. M. Blann, Phys. Rev. C 23, 205 (1981); C 31, 1245 (1985).

18. M. Blann, Nucl. Phys. A 235, 211 (1974); M. Blann, Proceedings of the International School on Nuclear Physics, Predeal, Romania 1974, ed. A. Ciocanel, p. 249, Bucharest (1976); M. Blann, A. Mignerey and W. Scobel, Nukleonika 21, 335 (1976).

19. N. Cindro, M. Korolija and E. Holub, "Fundamental Problems in Heavy Ion Collisions," ed. by N. Cindro, et al., p. 301, World Scientific, Singapore (1985).

20. G. Mantzouranis, H. A. Weidenmuller and D. Agassi, Z. Phys. A 276, 145 (1976).

21. M. Blann, W. Scobel and E. Plechaty, Phys. Rev. C 30, 1493 (1984).

22. C. B. Chitwood, et al., Phys. Rev. C 27, 447 (1983).

23. J. L. Laville, et al., Phys. Lett. 1568, 42 (1985); T. C. Awes, et al., Phys. Rev. C 24, 89 (1981).

24. G. F. Bertsch, Phys. Rev. C 15, 713 (1977).

25. M. Blann, Phys. Rev. C 32, 1231 (1985).

26. B. J. VerWest and R. A. Arndt, Phys. Rev. C 25, 1979 (1982).

This work was performed under the auspices of the U.S. Department of Energy by the Lawrence Livermore National Laboratory under contract number W-7405-ENG-48.